Polymer Chemistry

Accepted Manuscript

ROYAL SOCIETY OF CHEMISTRY

www.rsc.org/polymers

Journal Name

RSCPublishing

ARTICLE

Polymerization Induced Self-Assembly: Tuning of Nano-Object Morphology by Use of CO_2

Cite this: DOI: 10.1039/x0xx00000x

Received ooth January 2012,
Accepted ooth January 2012

DOI: 10.1039/x0xx00000x

www.rsc.org/

Siming Dong,[1] Wei Zhao,[2] Frank P. Lucien,[1] Sébastien Perrier,[3, 4] and Per B. Zetterlund [1,*]

Abstract: Polymeric nano-objects of non-spherical morphology (e.g. rods, vesicles) have a range of potential applications, and it is thus of great interest to develop synthetic approaches that enable large scale production as well as fine tuning of the morphology. To this end, we have developed reversible addition-fragmentation chain transfer (RAFT) dispersion polymerization in an alcoholic medium pressurized to low pressure (8.0 MPa) with CO_2. It is demonstrated that the presence of CO_2 has a profound effect on the morphology of the resulting polymer aggregates. In the presence of CO_2, the formation of nano-objects with a high interfacial core/corona curvature is favoured relative to the corresponding system without CO_2, e.g. rods are formed (with CO_2) under conditions where vesicles (no CO_2) would otherwise form. This is a convenient method for tuning the morphology without altering the recipe, and represents an attractive route to pure rod morphology, which is typically somewhat elusive.

Introduction

The self-assembly of molecules into nano-objects of various shapes is common in nature, as exemplified by formation of cell membranes by self-assembly of phospholipids. Such self-assembly can occur for species that comprise distinct hydrophobic and hydrophilic moieties, and is driven by minimization of the overall free energy of the system. The resulting aggregates can exhibit a wide range of morphologies, *e.g.* spherical micelles, worm-like micelles (rods), and vesicles. Self-assembly can also occur in the case of amphiphilic polymeric species, *e.g.* diblock copolymers, and the resulting aggregates are typically of higher stability than their low molecular weight (MW) counterparts (*e.g.* low MW surfactants).[1] As a consequence, polymeric self-assembled nano-objects have a range of potential applications in the fields of nanomedicine (*e.g.* drug delivery and imaging) microelectronics and catalysis,[2, 3] and there are currently significant research efforts directed towards development of facile means of synthesis as well as morphology control.

Polymeric nano-objects based on self-assembly are traditionally prepared via post-polymerization methods in dilute aqueous solutions (*e.g.* using dialysis), thus making large scale preparation of these materials a challenge. To this end, the relatively recently developed technique of polymerization induced self-assembly (PISA)[4-12] represents a very significant step forward in that it enables direct one-pot preparation of polymeric nano-objects of various morphologies in concentrated solutions. The method is based on controlled/living radical polymerization (CLRP)[13] in a dispersed system (emulsion or dispersion polymerization),[14] whereby self-assembly occurs as a result of controlled chain growth of a solvophobic block from a solvophilic block. A number of recent studies on PISA have resulted in detailed phase diagrams, outlining the conditions for formation of various specific nano-object morphologies.[15-17] However, despite this progress, it can be quite challenging to prepare non-spherical nano-objects of pure morphology for a given formulation, *e.g.* rods as opposed to a mixture of rods/vesicles. Rods/nanowires (*i.e.* rods of very high aspect ratio) are of great interest due to a number of potential applications, including templated synthesis of metal nano-objects and semiconductors,[18, 19] and enhanced drug delivery,[20] but unfortunately the experimental parameter space that yields pure rods via PISA can be quite narrow.[15]

In the present work, we have developed a method for tuning the nano-object morphology during PISA conducted via reversible addition-fragmentation chain transfer (RAFT[21, 22]) dispersion polymerization. It is demonstrated that pressurization of the system with CO_2 to low pressure in an easy to implement manner (~8 MPa), thus generating a gas expanded liquid,[23] has a profound effect on both polymerization rate and nano-object morphology.

Results and Discussion

A polymeric RAFT agent (M_n = 6,000 g/mol; $Đ$ = 1.07; the solvophilic block for the subsequent PISA process) was first prepared by polymerization of 4-vinylpyridine (4VP) in isopropanol at 90 °C initiated by 1,1'-azobis(cyclohexane-1-carbonitrile; V-40) using the low MW RAFT agent 2-cyano-2-propyl benzodithioate (CPBDT) (Scheme 1; Fig. S1). RAFT dispersion polymerizations (PISA) of styrene were subsequently conducted in isopropanol at 90 °C using V-40 as initiator employing the poly(4VP)-based macroRAFT agent with $[styrene]_0:[P4VP\text{-}CPBDT]_0:[V\text{-}40]_0$ = 5000:1:0.1 and styrene:isopropanol = 1:1 (wt:wt) (Scheme 1). All ingredients are soluble in the initial reaction mixture, but as the solvophobic polystyrene block reaches sufficient length, self-assembly into aggregates occurs. Initially, three polymerizations were conducted for 24 h: (*i*) No CO_2, and the system pressurized to (*ii*) 6.5 MPa and (*iii*) 8.0 MPa CO_2 using a specifically designed pressure reactor equipped with a viewing window.[24] When CO_2 was pressurized into the reactor (8.0 MPa), the volume of mixture expanded by a factor ~1.33 due to the dissolution of CO_2 in the liquid.

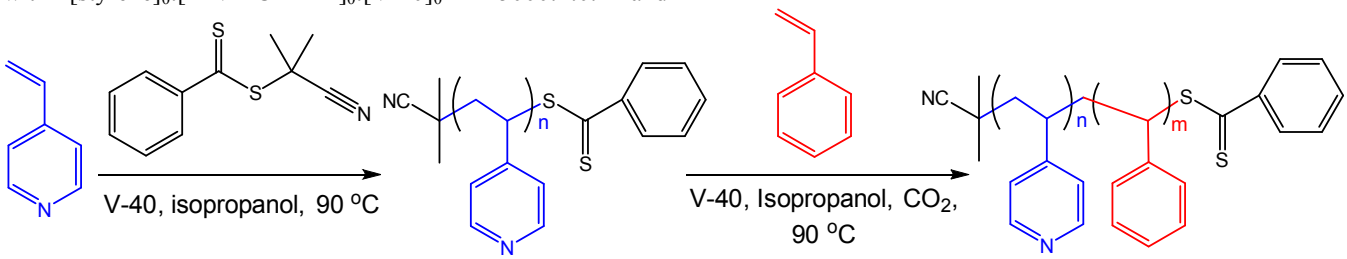

Scheme 1. Synthesis of P4VP-CPBDT macroRAFT agent and P4VP-*b*-PS by dispersion polymerization in CO_2-expanded isopropanol.

TEM imaging of the resultant nano-objects reveals very different morphologies; vesicles were obtained without CO_2, whereas rods and rods/spheres were obtained at 6.5 and 8.0 MPa, respectively （Fig. 1). For a given set of conditions, an increase in the length of the solvophobic block (styrene block) leads to morphology transitions in the order spheres-rods-vesicles.[4-12] Given that DP_n (6.5 MPa) > DP_n (no CO_2), it appears that CO_2 directly influences the morphology. The sample at 8.0 MPa did have somewhat lower DP_n than the sample without CO_2, and it can thus not be concluded that the presence of CO_2 in this case caused the morphology change from vesicles to spheres/rods. It is interesting to note that on CO_2 depressurization, the morphology does not revert back to the corresponding non-CO_2 morphology. These initial data thus suggest that the presence of CO_2 causes a "delay" in morphology development that is equivalent to reducing the length of the solvophobic block.

	No CO_2	6.5 MPa	8.0 MPa
DP_n	205	222	172
$Đ$	1.40	1.15	1.11

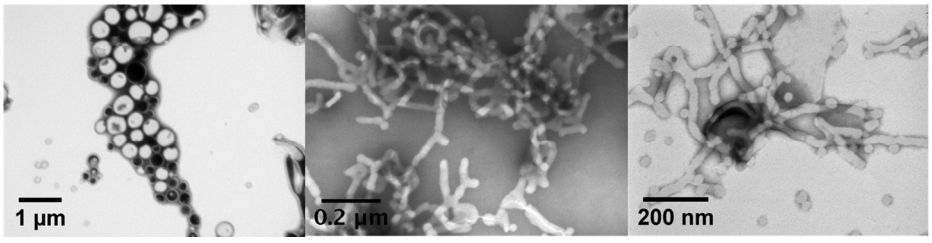

Figure 1. Number-average degrees of polymerization (DP_n), dispersity ($Đ$) values and TEM images at different CO_2 pressures for dispersion polymerization of styrene using a P4VP macroRAFT agent in isopropanol at 90 °C for 24 h.

To carefully map out the morphology transitions with conversion, polymerizations were monitored over time with (8.0 MPa) and without CO_2 using the experimental conditions above. Conversion-time data (Fig. S4) reveal that the polymerization rate was reduced by a factor of ~2 in the presence of CO_2. Similar retardative effects of CO_2 have been reported previously for the conventional (not CLRP) radical dispersion polymerization of styrene, attributed to increased partitioning of styrene from particles to the continuous phase[25] (the former being the main locus of polymerization, and the sole locus in case of dispersion CLRP once particles have formed). Prior to particle formation, a rate decrease would be expected simply based on dilution effects on expansion with CO_2. In the present systems (with and without CO_2), the dynamic light scattering (DLS) data in Fig. 6 (discussed below) indicate that particles appear to be present at 2h (no CO_2) and 8h (CO_2), or before, corresponding to an onset of particle formation at conversions below 3-4% (Fig. S3). Both with and

without CO_2, the MW distributions remained narrow and shifted to higher MW with increasing conversion (Fig. S2), and the M_n values increased close to linearly with conversion (Fig. 2) as expected in a controlled/living system. Interestingly, the M_n values were consistently higher with CO_2 than without at a given conversion, and $M_n < M_{n,th}$ both with and without CO_2 for reasons that remain to be clarified. The $Đ$ values were relatively similar for both systems, remaining below 1.4 (Fig. 2).

The morphology was examined via TEM (Fig. 3), revealing clear differences between the two systems. Consistent with the data presented in Fig. 1, the morphology transitions were "delayed" in the presence of CO_2, and under the current CO_2 conditions never reached the vesicle stage (unlike without CO_2). Under the current conditions, significantly higher conversion than 8-10% cannot be reached in the present system, partly due to the fact that that the initiator V-40 has a 10-hour half-life temperature of 88 °C, and as such the rate of initiation will be very low after ~30 h. Without CO_2, the transition from spheres to rods occurred in the number-average degree of polymerization (DP_n) range 21-89, and vesicles started to appear at DP_n values beyond 115. In the CO_2 system, spheres remained until $DP_n \approx 127$, and rods only started to appear around $DP_n \approx 118$. At $DP_n \approx 204$, pure rods where formed (Fig. 3). Preliminary experiments using another recipe/conditions that favour vesicle formation demonstrated that the rods-vesicle transition can occur also in the presence of CO_2.

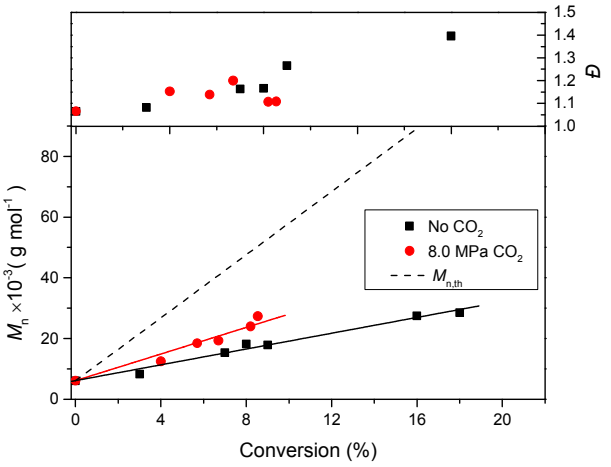

Figure 2. Evolution of molecular weights and dispersities ($Đ$) with conversion for dispersion polymerization of styrene using a P4VP macroRAFT agent in isopropanol at 90 °C without CO_2 and at a CO_2 pressure of 8.0 MPa. The dotted line shows $M_{n,th}$.

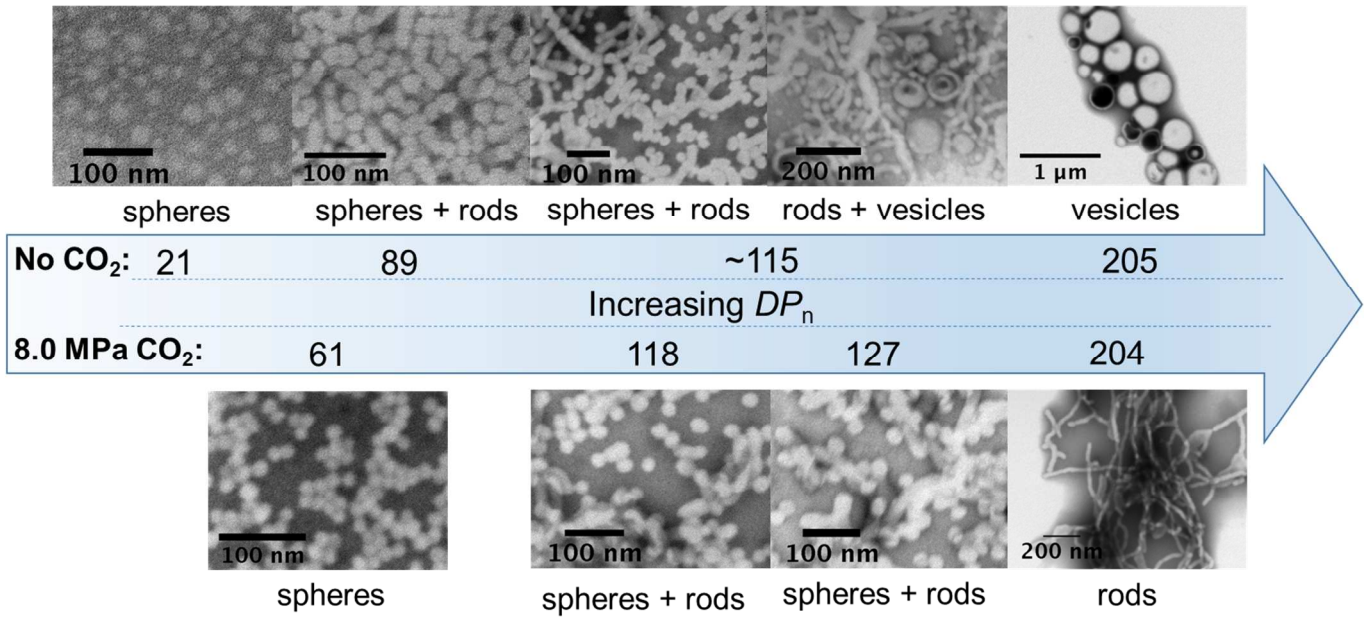

Figure 3. TEM images showing the morphologies of dispersion polymerization of styrene using a P4VP macro RAFT agent in isopropanol at 90 °C without CO_2 and at a CO_2 pressure of 8.0 MPa at different polymerization times (degrees of polymerization shown in the blue arrow).

In addition to examining the morphology via TEM, online DLS measurements were conducted whereby the scattering intensity was measured over 1 h time intervals as a function of time for both systems (*i.e.* without depressurizing the system in case of 8.0 MPa CO_2; Fig. S5; For experimental details and further discussion, see Supplementary Information). Online DLS monitoring is a unique and powerful technique to observe structure change in particles during polymerization. It is however of limited meaning to compare scattering data vs time, given that the two systems exhibit growth of the solvophobic block at different rates. The scattering vs time data were thus transformed to scattering vs conversion data as well as

scattering vs. number-average degree of polymerization (DP_n) of solvophobic block by fitting polynomials to the conversion-time (Fig. S4) and DP_n-time (Fig. S3) data, respectively. The thus obtained scattering intensity vs DP_n and scattering intensity vs conversion plots (Fig. 4) demonstrate that there is indeed a very significant effect of CO_2. In both plots, with the exception of the lowest conversion/DP_n range, the scattering intensity values are consistently lower in the presence of CO_2 than without. This is mainly attributed to the delayed onset of formation of the higher order structures rods and vesicles in the presence of CO_2, as already indicated in Fig. 1. The onset of the transition from spheres to rods is particularly apparent in the presence of CO_2, in which case the scattering intensity remains close to constant until $DP_n \approx 120$, after which there is a marked increase (consistent with TEM images).

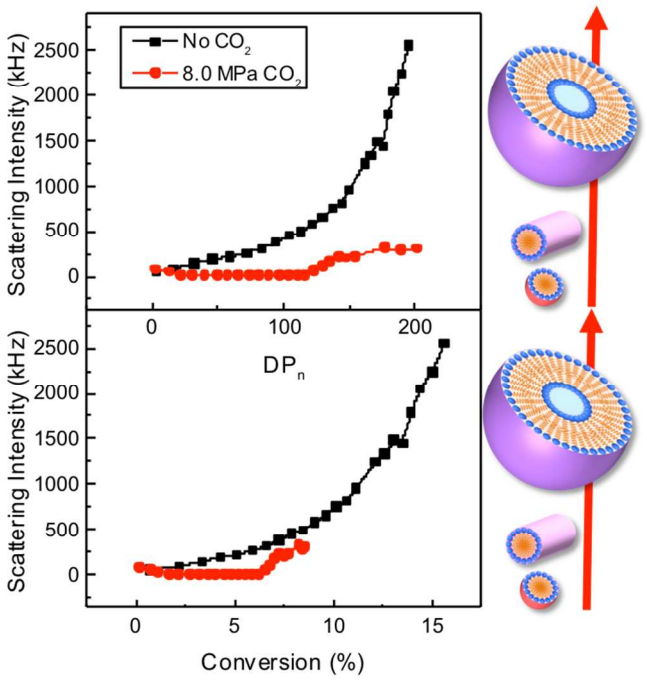

Figure 4. Online DLS scattering intensity vs. DP_n/conversion measured *in situ* for RAFT dispersion polymerization of styrene using a P4VP macroRAFT agent in isopropanol at 90 °C without CO_2 and at a CO_2 pressure of 8.0 MPa

Fig. 5 shows the evolution of morphology during the polymerization in terms of DP_n vs polymerization time for the two systems based on TEM images and the DLS scattering intensity data (see Supporting Information for details). Two points are to be highlighted: (*i*) The morphology transitions are delayed in the presence of CO_2, and (*ii*) rods are more easily accessible in the presence of CO_2 because of the wider "window" of each morphology.

In addition, the average size of aggregates at different polymerization times was investigated by offline DLS (Fig. 6). The particle size increased with time for both systems, consistent with the morphology changing from spheres to rods and then from rods to vesicles in the absence of CO_2, and from spheres to rods in the presence of CO_2. It can be observed that, in a comparable DP_n range, the size of self-assembly aggregates formed in the presence of CO_2 is smaller than without CO_2.

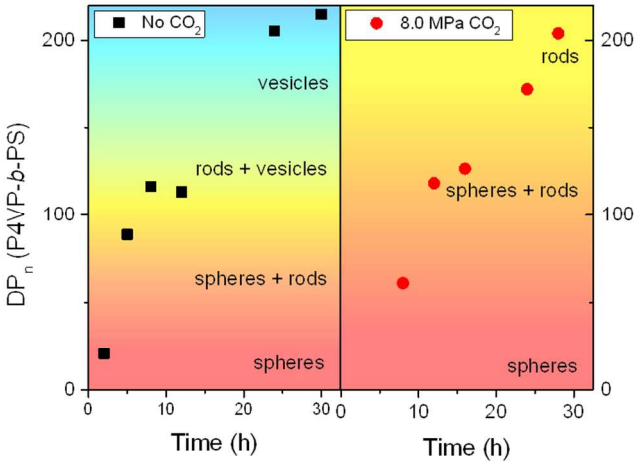

Figure 5. Evolution of morphology during the polymerization in terms of DP_n vs polymerization time for RAFT dispersion polymerization of styrene using a P4VP macroRAFT agent in isopropanol at 90 °C without CO_2 and at a CO_2 pressure of 8.0 MPa

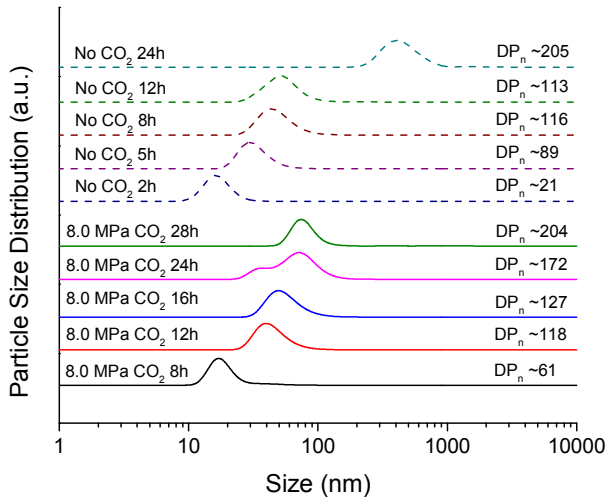

Figure 6. Number-based particle size distributions and number average degrees of polymerization (DP_n) for RAFT dispersion polymerization of styrene using a P4VP macroRAFT agent in isopropanol at 90 °C without CO_2 and at a CO_2 pressure of 8.0 MPa.

The effect of CO_2 was also examined in dispersion polymerizations of styrene in another solvent system - ethanol/water (8:1 weight ratio) - without CO_2 and at a CO_2 pressure of 6.5MPa using another P4VP macroRAFT agent (M_n = 13,800; $Đ$ = 1.08). Without CO_2, vesicles were formed after 8h, corresponding to $DP_n \approx 218$, while at 6.5 MPa of CO_2, only rods were observed after 24h at $DP_n \approx 547$, (Fig. 7). The phase transition from rods to vesicles was thus again markedly delayed in the presence of CO_2.

Run	Pressure (MPa)	M_n	DP_n	$Đ$	Morphology
1	No CO_2 (8h)	36500	218	1.05	Vesicles
2	6.5 (24h)	70700	547	1.15	Rods

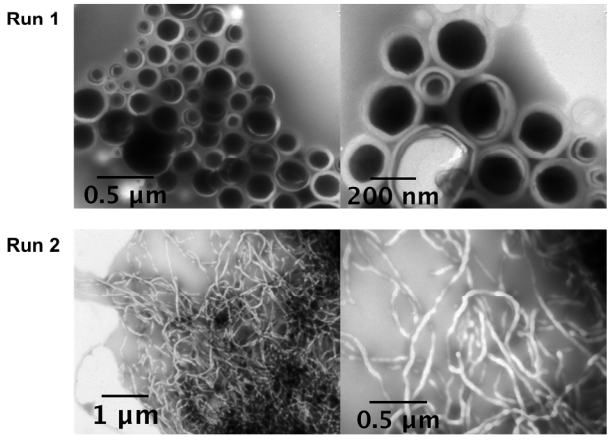

Figure 7. Molecular weight (M_n), DP_n, dispersity ($Đ$) values and TEM images for dispersion polymerization of styrene using a P4VP macroRAFT agent in ethanol/water (8:1) at 90 °C without CO_2 and at a CO_2 pressure of 6.5 MPa

Further work is required to clarify the exact mechanism(s) involved in the effect(s) of CO_2 on these systems. Four mechanisms may be at play: (*i*) In the presence of CO_2, increased partitioning of styrene to the continuous phase occurs, causing reduced mobility of chain segments in the core, thus preventing rod to vesicle transition from occurring (Scheme 2). This effect of CO_2 has previously been observed in heterogeneous polymerizations in CO_2-expanded solvents.[24, 25] Similar effects have also been reported for traditional RAFT PISA systems without CO_2 – use of a solvent mixture that swells the core less tends to shift morphology from vesicles towards rods and spheres.[15, 26] However, unlike CO_2-expanded solvents, the properties of which can be easily tuned via the control of pressure, such flexibility can be less accessible via simple mixing of solvents. In addition, CO_2-expanded solvents provide enhanced safety with regards to flammability.

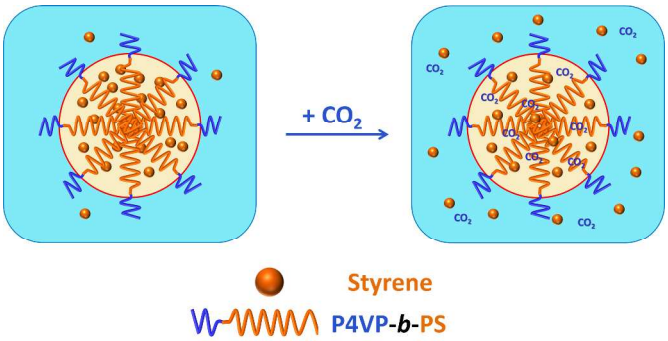

Scheme 2. Increased partitioning of styrene from the dispersed phase (light yellow colour) to the continuous phase (light blue colour) in the presence of CO_2

(*ii*) Dense CO_2 is essentially a non-polar solvent, and consequently it is anticipated that CO_2-expanded isopropanol/styrene would be less polar than pure isopropanol/styrene, and therefore a better solvent for the solvophobic polystyrene block.[25] This would have the effect of shifting the morphology transitions to higher degrees of polymerization of styrene. (*iii*) Due to volumetric expansion with CO_2, the block copolymer concentration decreases, which is known to shift morphologies in the direction of spheres.[1, 27] In this case, the initial volumetric expansion at a CO_2 pressure of 8.0 MPa is approximately a factor of 1.33, which leads to a reduction in aggregate concentration by ~25%. (*iv*) In the aqueous-based system, the presence of CO_2 leads to a reduction in pH, which causes protonation of 4VP units of the corona. This in turn would lead to increased repulsion between corona chain, thus making it less energetically favorable for morphologies with low interfacial curvature (*i.e.* higher order structures like rods and vesicles) to form.[1, 28, 29]

Conclusions

To summarize, we have developed a method for synthesis of polymeric nano-objects via polymerization-induced self-assembly in a CO_2-expanded medium. The main advantages of this approach are that one can tune the morphology continuously using CO_2 without altering the polymerization recipe, and that the typically elusive pure rod-morphology, which is interesting due to a range of promising applications of such nano-objects, is more accessible in the presence of CO_2.

Notes and references

[1] Centre for Advanced Macromolecular Design (CAMD), School of Chemical Engineering, The University of New South Wales, Sydney, NSW 2052, Australia
[2] Key Centre for Polymers & Colloids, School of Chemistry, The University of Sydney, New South Wales 2006, Australia
[3] Department of Chemistry, The University of Warwick, Gibbet Hill, Coventry, CV4 7AL, United Kingdom
[4] Faculty of Pharmacy and Pharmaceutical Sciences, Monash University, 381 Royal Parade, Parkville, VIC 3052, Australia

Electronic Supplementary Information (ESI) available: [details of any supplementary information available should be included here]. See DOI: 10.1039/b000000x/

1. Y. Y. Mai and A. Eisenberg, *Chem. Soc. Rev.*, 2012, **41**, 5969-5985.
2. G. Riess, *Prog. Polym. Sci.*, 2003, **28**, 1107-1170.
3. H. Lomas, I. Canton, S. MacNeil, J. Du, S. P. Armes, A. J. Ryan, A. L. Lewis and G. Battaglia, *Adv. Mater.*, 2007, **19**, 4238-+.
4. W.-M. Wan, C.-Y. Hong and C.-Y. Pan, *Chem. Commun.*, 2009, 5883-5885.
5. W. M. Wan and C. Y. Pan, *Polym. Chem.*, 2010, **1**, 1475-1484.
6. N. J. Warren and S. P. Armes, *J. Am. Chem. Soc.*, 2014, **136**, 10174-10185.
7. J.-T. Sun, C.-Y. Hong and C.-Y. Pan, *Polym. Chem.*, 2013, **4**, 873-881.
8. B. Charleux, G. Delaittre, J. Rieger and F. D'Agosto, *Macromolecules*, 2012, **45**, 6753-6765.

9. W. Zhao, G. Gody, S. Dong, P. B. Zetterlund and S. Perrier, *Polym. Chem.*, 2014, **5**, 6990-7003.
10. C. Gonzato, M. Semsarilar, E. R. Jones, F. Li, G. J. P. Krooshof, P. Wyman, O. O. Mykhaylyk, R. Tuinier and S. P. Armes, *J. Am. Chem. Soc.*, 2014, **136**, 11100-11106.
11. X. W. Zhang, S. Boisse, W. J. Zhang, P. Beaunier, F. D'Agosto, J. Rieger and B. Charleux, *Macromolecules*, 2011, **44**, 4149-4158.
12. J. T. Sun, C. Y. Hong and C. Y. Pan, *Soft Matter*, 2012, **8**, 7753-7767.
13. W. A. Braunecker and K. Matyjaszewski, *Prog. Polym. Sci.*, 2007, **32**, 93-146.
14. P. B. Zetterlund, Y. Kagawa and M. Okubo, *Chem. Rev.*, 2008, **108**, 3747-3794.
15. A. Blanazs, A. J. Ryan and S. P. Armes, *Macromolecules*, 2012, **45**, 5099-5107.
16. N. J. Warren, O. O. Mykhaylyk, D. Mahmood, A. J. Ryan and S. P. Armes, *J. Am. Chem. Soc.*, 2014, **136**, 1023-1033.
17. B. Karagoz, L. Esser, H. T. Duong, J. S. Basuki, C. Boyer and T. P. Davis, *Polym. Chem.*, 2014, **5**, 350-355.
18. J. Y. Yuan and A. H. E. Muller, *Polymer*, 2010, **51**, 4015-4036.
19. Y. Y. Mai and A. Eisenberg, *Macromolecules*, 2011, **44**, 3179-3183.
20. Y. Geng, P. Dalhaimer, S. S. Cai, R. Tsai, M. Tewari, T. Minko and D. E. Discher, *Nat. Nanotech.*, 2007, **2**, 249-255.
21. S. Perrier and P. Takolpuckdee, *J. Polym. Sci.; Part A: Polym. Chem.*, 2005, **43**, 5347-5393.
22. G. Moad, E. Rizzardo and S. H. Thang, *Aust. J. Chem.*, 2012, **65**, 985-1076.
23. P. G. Jessop and B. Subramaniam, *Chemical Reviews*, 2007, **107**, 2666-2694.
24. D. Pu, F. P. Lucien and P. B. Zetterlund, *J. Polym. Sci.; Part A: Polym. Chem.*, 2011, **49**, 4307-4311.
25. D. W. Pu, M. P. Devitt, S. C. Thickett, F. P. Lucien and P. B. Zetterlund, *Polymer*, 2013, **54**, 6689-6694.
26. X. W. Zhang, J. Rieger and B. Charleux, *Polym. Chem.*, 2012, **3**, 1502-1509.
27. L. F. Zhang and A. Eisenberg, *Macromolecules*, 1999, **32**, 2239-2249.
28. S. Boissé, J. Rieger, G. Pembouong, P. Beaunier and B. Charleux, *J. Polym. Sci., Part A: Polym. Chem.*, 2011, **49**, 3346-3354.
29. M. Semsarilar, V. Ladmiral, A. Blanazs and S. P. Armes, *Langmuir*, 2013, **29**, 7416-7424.